

## Influence of Process Parameters Variation on Microstructure and Mechanical Properties of SLM-Printed 316L Stainless Steel

Mike T. Hauschultz<sup>1,a\*</sup>, Maria H. Friedo<sup>1,b</sup>, Ute Geissler<sup>1,c</sup>, Andrea Böhme<sup>1,d</sup>  
and René Krenz-Baath<sup>1,e</sup>

<sup>1</sup>Technical University of Applied Sciences Wildau, Hochschulring 1, 15745 Wildau, Germany

<sup>a</sup>mike.hauschultz@th-wildau.de, <sup>b</sup>maria\_helene.friedo@th-wildau.de, <sup>c</sup>ute.geissler@th-wildau.de,  
<sup>d</sup>andrea.boehme@th-wildau.de, <sup>e</sup>rene.krenz-baath@th-wildau.de

**Keywords:** 316L stainless steel, additive manufacturing, selective laser melting, parameter optimization.

**Abstract.** This study presents the characterization of 316L stainless steels fabricated by selective laser melting (SLM), focusing on the influence of printing parameters on microstructure and mechanical properties. The choice of process parameters is crucial for achieving desired material properties, as it directly affects the microstructure and mechanical behavior, which is important when optimizing for potential applications in several fields, such as aerospace and automotive. In this study, different scanning speeds were tested to identify optimal settings, followed by the evaluation of the effects of orientation relative to the build plate and hatching strategies to enhance performance. To assess the impact of these factors, tensile tests, microhardness measurements, and X-ray diffraction (XRD) analyses were conducted. Tensile tests revealed that higher laser scanning speed generally reduces ultimate tensile strength and elongation, likely due to an increase in porosity and a less homogeneous fusion of layers. The analysis of samples printed with different orientation relative to the build plate highlighted a strong mechanical anisotropy, with the samples printed vertically exhibiting lower tensile strength and ductility compared to horizontally printed samples. Microhardness testing further confirmed an anisotropy in material properties. XRD analysis reveals a preferential orientation of austenitic grains depending on building direction. This, in turn, influences the anisotropic behavior. These findings highlight the critical role of process parameters in tailoring the microstructure and mechanical performance of SLM-produced parts, thereby providing insights into the optimization of additive manufacturing for specific applications.

### Introduction

This study marks the beginning of a broader research initiative on process optimization for 316L stainless steel using the Selective Laser Melting (SLM) process. 316L has achieved industrial relevance in marine and automotive applications due to its exceptional corrosion resistance, favorable mechanical properties, high-temperature strength and non-magnetic properties [1].

SLM itself offers distinct benefits over conventional manufacturing techniques. It allows for complex inner and outer geometries that are not feasible through subtractive manufacturing. This approach has the potential to result in a substantial reduction in material usage and waste, thereby offering significant environmental benefits. Despite the necessity of filling the entire build platform during the SLM process, the residual powder can be reused, thereby circumventing the generation of waste. However, this process and the properties of the created parts are highly dependent on the choice of process parameters. This can result for example in elevated internal stresses [1]. Advantageously, this dependency can be used to modify the properties in specific features. This process necessitates a comprehensive understanding of the correlation between parameters, properties and application. This study shall contribute to this deeper understanding through tensile tests, hardness measurements and X-ray diffraction (XRD) analysis of parameter varied parts.

## Materials and Methods

All the examined specimens were produced using the SLM machine MPrint+ from the supplier One Click Metal. It offers a build volume of  $(150 \text{ mm})^3$  using a continuous-wave fiber laser that operates at  $1080 \pm 5 \text{ nm}$  with a maximum output power of 200 W. The powder used is 316L stainless steel (d10:  $21 \mu\text{m}$ , d50:  $32 \mu\text{m}$ , d90:  $44 \mu\text{m}$ ) provided by metals4printing.

The parameter variations were executed as single-parameter variations from a baseline parameter set which consists of a laser power of 200 W, an 800 mm/s scanning speed and a hexagonal hatching pattern with a hatching distance of 0.1 mm. The variations that were tested included scanning speeds from 400 mm/s to 1600 mm/s in 200 mm/s increments, build orientations of  $0^\circ$ ,  $45^\circ$  and  $90^\circ$  towards the build plate and various hatching patterns (hexagon, quad, stripe, meander) (Fig. 1 a – d).

The present study examined the influence of scanning speed and inclination on tensile strength using test specimens according to DIN EN ISO 6892-1 (form A, 6 mm diameter, 36 mm parallel length). The specimens were printed in an oversize format and then machined to final diameter using a lathe. They were tested until ultimate failure using a TIRAtest 24100 universal testing machine, upgraded with a Zwick measurement system, accompanied by the software testXpert V11.02 Master.

The effects of hatching pattern on microhardness (HV0.05) and X-ray diffraction (XRD) were examined using plate-shaped samples of 50 mm x 50 mm x 5 mm dimension which were fabricated in  $0^\circ$ ,  $45^\circ$  and  $90^\circ$  inclination (Fig. 1 e – f). The XRD analysis of the samples was conducted using a Philips diffractometer PW1729 in comparison to a JCPDS standard.

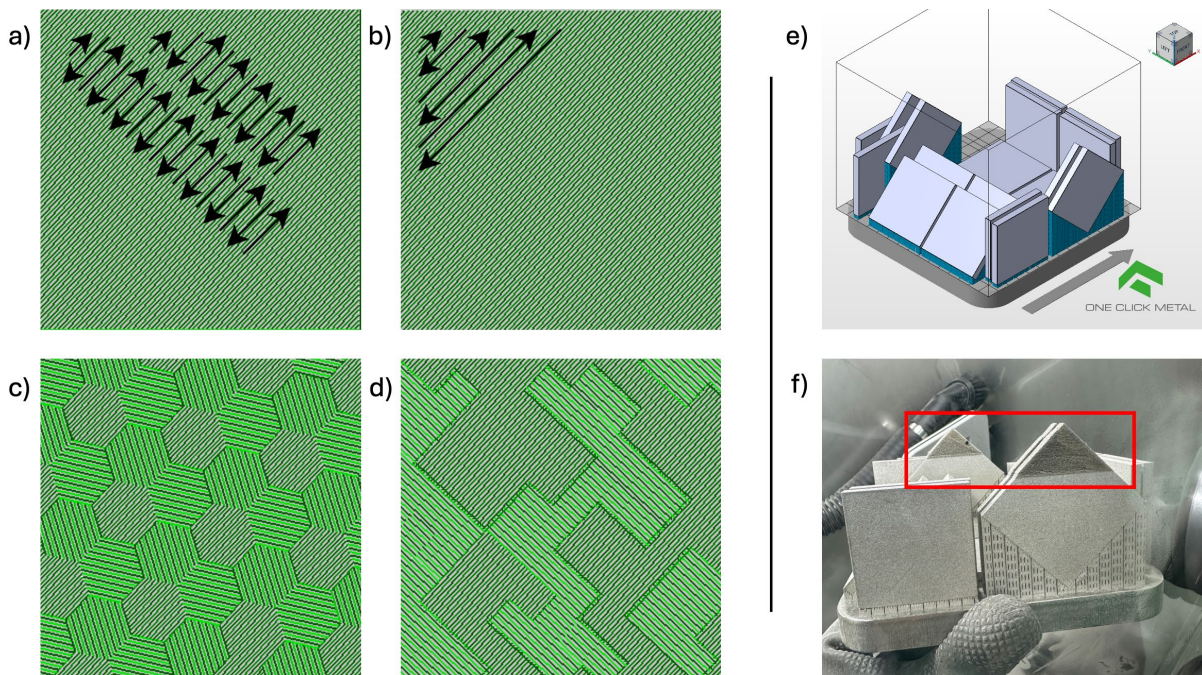


**Fig. 1.** Sample preparation for Vickers microhardness measurements and XRD analysis. Hatching patterns: a) stripe, b) meander, c) hexagon, d) quad. Build plate setup: e) print preparation in Autodesk Netfabb 2025, coating direction indicated by grey arrow, f) print result: ( $90^\circ$ ,  $45^\circ$ ,  $0^\circ$ ) orientation could not be used for examination due to restricted gas flow.

## Results and Discussion

The results are presented in three parts: the influence of (i) the build orientation and (ii) the scanning speed on the tensile strength and (iii) the influence of hatching pattern on microhardness and XRD.

### Influence of Build Orientation.

As illustrated in Fig. 2 the building direction is closely linked to the appearance of the stress-strain curves. The specimens that were fabricated horizontally exhibited the highest ultimate tensile strength (UTS) at  $701.52 \pm 2.75 \text{ MPa}$ , with the  $45^\circ$  specimens exhibiting slightly lower UTS at  $690.12$

$\pm 0.87$  MPa. The specimens that were printed vertically exhibit a 14%, respective 12%, lower UTS at  $605.94 \pm 0.88$  MPa. This behavior is indicative of pronounced mechanical anisotropy.

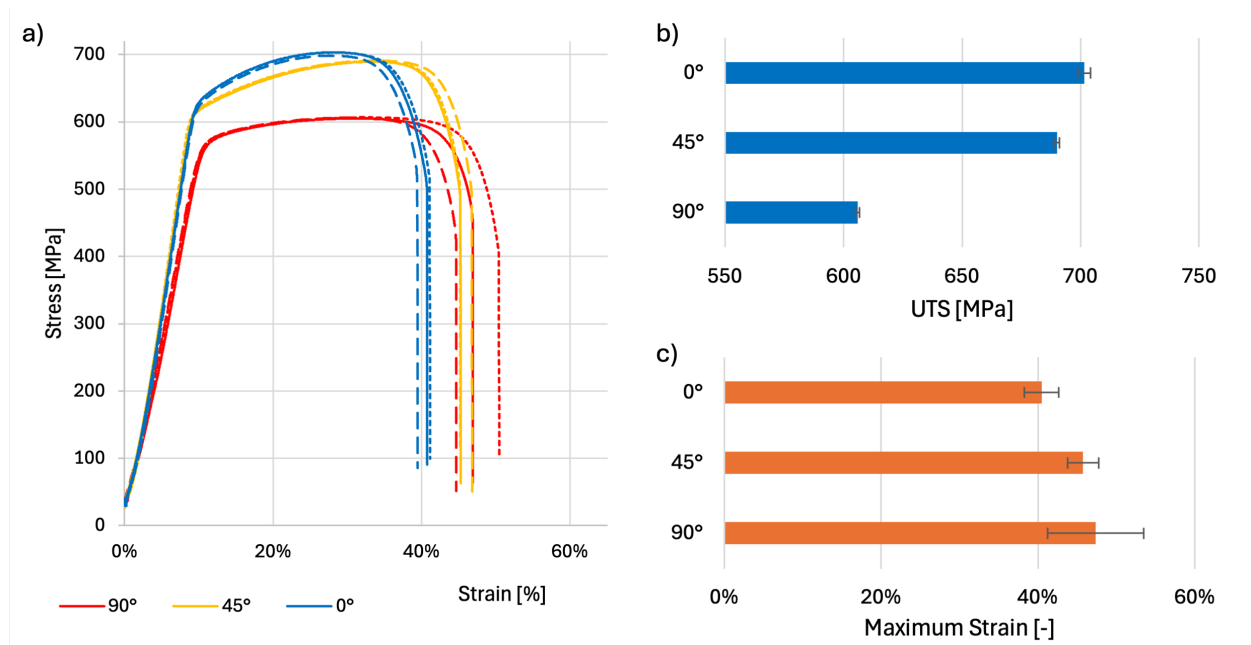


**Fig. 2.** Results of tensile tests regarding printing orientation towards build plate. a) Stress-strain-curves, b) ultimate tensile strength of sample groups, c) maximum strain of sample groups.

An opposite behavior was observed for the maximum strain of the same samples. The 0° specimens demonstrated the lowest elongation with an average of 40.45%. The highest elongation and standard deviation were measured for the 90° samples at  $47.34 \pm 6.14\%$ . The results, especially the difference between 0° and 90°, are comparable to the findings of analogous studies [2,3]. The observed decrease in performance at 45° compared to 0° conversely deviates from prior published works [3] that reported slightly higher UTS for 45°. This anisotropic behavior can be attributed to the bidirectional cooling effects along the scanning path and in the melt pools from border to center which leads to the well-known “fish-scale pattern” (Fig. 3) of melt pools [4]. This alignment of substructures along the melt pool boundaries (MPB) plays a direct mechanical role. As demonstrated by Zhou et al. [5], the application of load parallel to the MPB enables greater deformation before breaking whereas perpendicular forces result in earlier tearing.

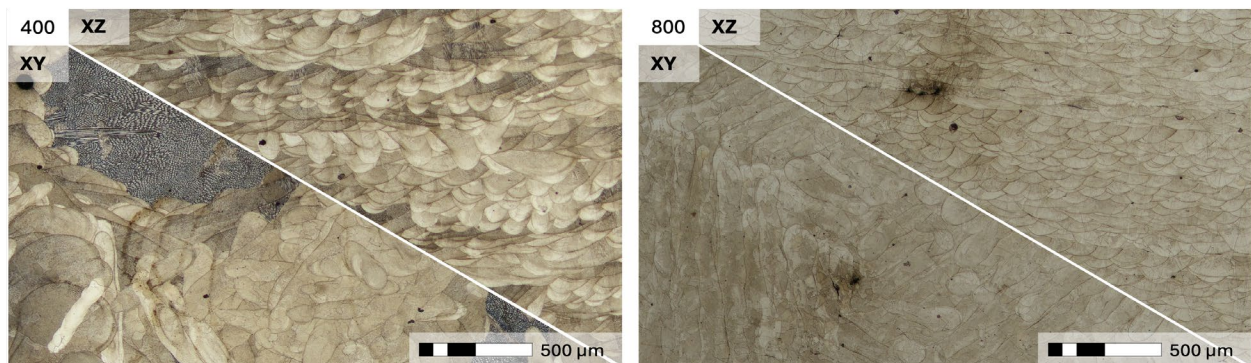


**Fig. 3.** As-printed SLM microstructure of scanning speed samples (400 mm/s, 800 mm/s). Each polished and etched along XY plane and XZ plane. Laser scanning speed is indicated in top left.

### Influence of Scanning Speed.

The impact of scanning speed was analyzed in the evolving microstructure and in tensile tests. A highly anisotropic microstructure containing the well-known melt pool pattern is evident in all micrographs (Fig. 3, 4), corresponding to the mechanical properties shown in Fig. 2.



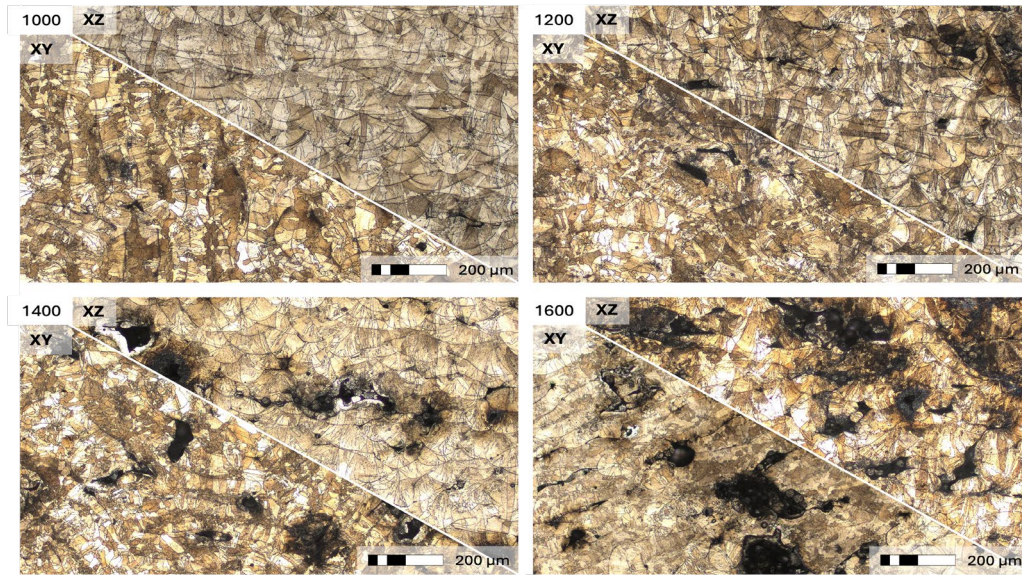


**Fig. 4.** As-printed SLM microstructure of scanning speed samples (1000 mm/s – 1600 mm/s). Each polished and etched along XY plane and XZ plane. Laser scanning speed is indicated in top left.

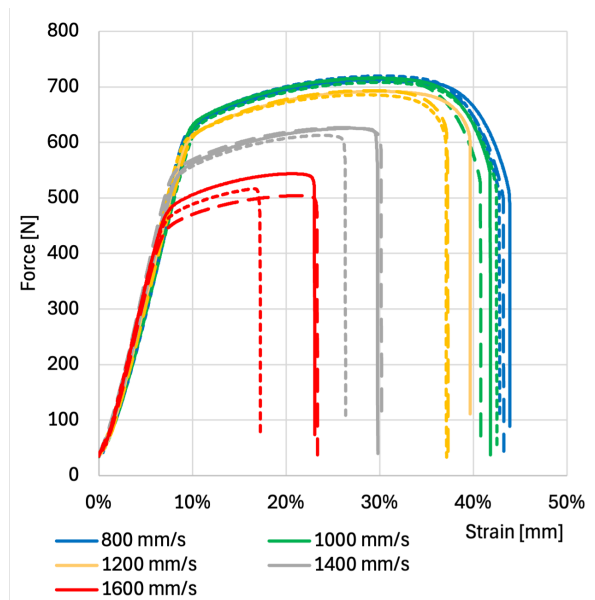


**Fig. 5.** Results of tensile tests regarding scanning speed towards build plate.

In specimens processed at scanning speeds as low as 400 mm/s, millimeter-scale gray zones were observed (Fig. 3). Segregation is well-known for SLM applications on a micrometer scale [6], but due to their bigger size, these observed gray zones cannot be attributed to elemental segregation alone. Instead, they point to macrostructural effects of overheating, including phenomena such as localized grain coarsening, porosity and oxidation. As this work reflects early-stage process development, further studies including EBSD and EDX are planned.

As scanning speeds are increased (Fig. 4), the side (XZ) and top (XY) views of the melt pool structure clearly illustrate the development of porosity. At a velocity of 1000 mm/s, a well-formed, SLM-typical fish-scale pattern is visible, exhibiting only minor imperfections. As the scanning speed increases further, porosity becomes more pronounced, particularly in the form of lack-of-fusion pores. At a scanning rate of 1600 mm/s, porosity is extensive, indicating that insufficient energy input prevents complete melting and consolidation.

The aforementioned visual irregularities are reflected in the mechanical properties of the tensile specimens fabricated using the same parameters. While tensile strength at 800 mm/s and 1000 mm/s are comparable (Fig. 5), samples fabricated at higher scanning speeds exhibit earlier failure at lower strains and more abrupt force drops after the peak. This finding suggests a transition toward a more brittle failure mode.

### Influence of Hatching Pattern.

Finally, the influence of the hatching pattern, in conjunction with the build orientation, was examined using microhardness measurements and XRD.

The microhardness HV0.05 (Fig. 6) demonstrates dependencies on inclination and on the hatching pattern. The influence of inclination appears to be more significant, as horizontally built samples exhibit the highest degree of hardness, followed by samples produced at a 45° inclination. The influence of the hatching pattern is smaller but still measurable. A notable consistency between the measured HV0.05 and published HV0.2 values [7] has been observed suggesting that the material exhibits minimal variation in hardness across different structural levels.

The results of the XRD analysis are displayed in Fig. 7. In this case, similar to the microhardness measurements, a strong correlation is evident between inclination and texture coefficient. The hatching pattern, on the other hand, is found to be of secondary importance.

The vertically built plates (90°, 0°, 0°) showed pronounced  $\gamma$ 200 and  $\gamma$ 400 texture components. These components indicated strong preferential grain orientation within a cubic crystal structure. The 45° samples demonstrated a diminished overall texture, exhibiting a reduction in  $\gamma$ 200 components. The presence of enhanced  $\gamma$ 220 peaks, suggesting strong crystallographic alignment along this plane, is evident for the horizontally built plates. This observation indicates the presence of a {110} <001> Goss texture [8,9], which is commonly associated with directional solidification under steep thermal gradients. This condition is consistent with SLM, as it exhibits cooling rates as high as 10<sup>6</sup> K/s [10].

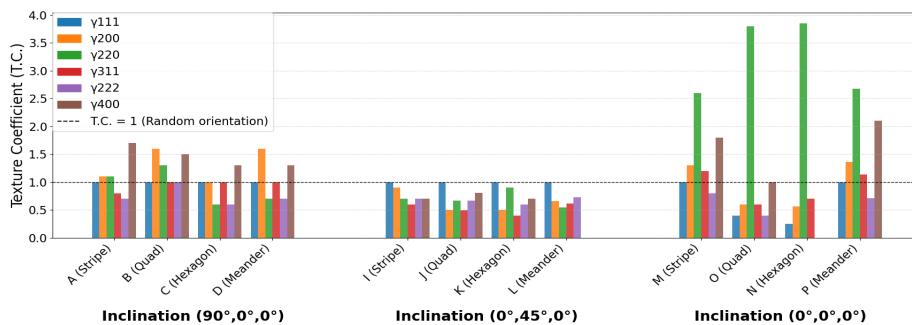


**Fig. 7.** Texture coefficients (T.C.) of various SLM-fabricated samples, evaluated for six crystallographic planes. Samples differ in build orientation and hatch strategy. A random texture corresponds to T.C. = 1 (dashed line); deviations indicate preferred crystallographic orientation.

### Conclusion and Outlook

The present study investigated the influence of process parameters and build orientation on the mechanical and microstructural properties of SLM-manufactured 316L stainless steel. Results such as highly anisotropic mechanical properties and scanning speed-dependent porosity are in good

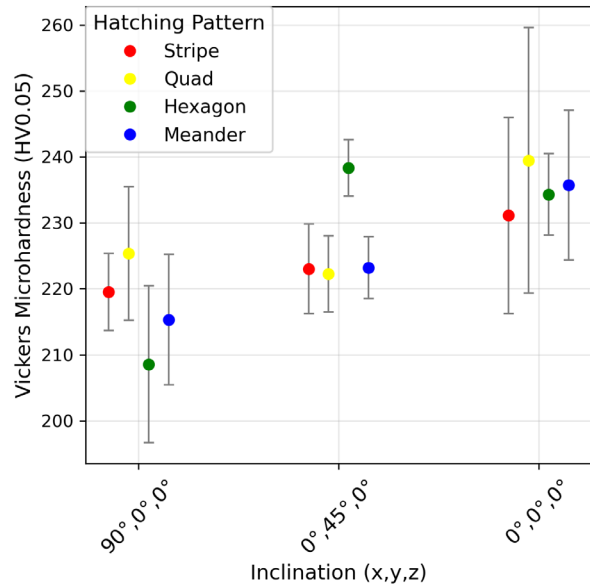


**Fig. 6.** Vickers microhardness measurements (HV0.05) of samples, produced using various hatching strategies and different inclinations.

agreement with existing literature. However, other observations-such as the appearance of millimeter-scale gray zones-require further investigation, for example using EBSD or EDX. The findings indicate that using a laser power of 200 W and a hatching distance of 0.1 mm, in conjunction with a scanning rate between 800 mm/s and 1000 mm/s yielded optimal results. The impact of orientation on mechanical properties and texture is more significant than that of hatching pattern.

This study represents the first phase of a broader investigation. Further examination is necessary to ascertain the impact of additional parameters on the final built components. Examples of such parameters include hatching distance, laser power and layer thickness which at least partially need to be combined with those parameters already studied. Further interest lies in examining various post-processing techniques and the general impact on dimensional accuracy and stability. Subsequent to the completion of these investigations, the objective is to implement this optimization method in another material to ensure its validity. In an ideal scenario, these results could be adapted for implementation in the context of in-process monitoring and control.

## References

- [1] Gao B, Zhao H, Peng L, Sun Z. A Review of Research Progress in Selective Laser Melting (SLM). *Micromachines (Basel)* 2022;14:57. <https://doi.org/10.3390/mi14010057>.
- [2] Thanumoorthy RS, Chaurasia JK, Anil Kumar V, Pradeep PI, Balan ASS, Rajasekaran B, Sahu A, Bontha S. Effect of Build Orientation on Anisotropy in Tensile Behavior of Laser Powder Bed Fusion Fabricated SS316L. *J Mater Eng Perform* 2024;33:7930–43. <https://doi.org/10.1007/s11665-023-08490-4>.
- [3] Li X, Yi D, Wu X, Zhang J, Yang X, Zhao Z, Wang J, Liu B, Bai P. Study on Mechanism of Structure Angle on Microstructure and Properties of SLM-Fabricated 316L Stainless Steel. *Front Bioeng Biotechnol* 2021;9. <https://doi.org/10.3389/fbioe.2021.778332>.
- [4] Zhang X, Yocom CJ, Mao B, Liao Y. Microstructure evolution during selective laser melting of metallic materials: A review. *J Laser Appl* 2019;31. <https://doi.org/10.2351/1.5085206>.
- [5] Zhou B, Xu P, Li W, Liang Y, Liang Y. Microstructure and Anisotropy of the Mechanical Properties of 316L Stainless Steel Fabricated by Selective Laser Melting. *Metals (Basel)* 2021;11:775. <https://doi.org/10.3390/met11050775>.
- [6] Yeganeh M, Shahryari Z, Talib Khanjar A, Hajizadeh Z, Shabani F. Inclusions and Segregations in the Selective Laser-Melted Alloys: A Review. *Coatings* 2023;13:1295. <https://doi.org/10.3390/coatings13071295>.
- [7] Zhao L, Zhang J, Yang J, Hou J, Li J, Lin J. Microstructure and mechanical properties of 316L stainless steel manufactured by multi-laser selective laser melting (SLM). *Materials Science and Engineering: A* 2024;913:147053. <https://doi.org/10.1016/j.msea.2024.147053>.
- [8] Andreau O, Koutiri I, Peyre P, Penot J-D, Saintier N, Pessard E, De Terris T, Dupuy C, Baudin T. Texture control of 316L parts by modulation of the melt pool morphology in selective laser melting. *J Mater Process Technol* 2019;264:21–31. <https://doi.org/10.1016/j.jmatprotec.2018.08.049>.
- [9] Puichaud A-H, Flament C, Chniouel A, Lomello F, Rouesne E, Giroux P-F, Maskrot H, Schuster F, Béchade J-L. Microstructure and mechanical properties relationship of additively manufactured 316L stainless steel by selective laser melting. *EPJ Nuclear Sciences & Technologies* 2019;5:23. <https://doi.org/10.1051/epjn/2019051>.
- [10] Ma M, Wang Z, Zeng X. A comparison on metallurgical behaviors of 316L stainless steel by selective laser melting and laser cladding deposition. *Materials Science and Engineering: A* 2017;685:265–73. <https://doi.org/10.1016/j.msea.2016.12.112>.